Research Article / Review Article FUPRE JOURNAL 9(1):163-180(2025)

FUPRE Journal

of

Scientific and Industrial Research

ISSN: 2579-1184(Print) ISSN: 2578-1129 (Online)

http://fupre.edu.ng/journal

Effects of Antiretroviral Therapy (ART) on the Transmission Dynamics of HIV

OKEDOYE, M. A. [1,*], ***FATAI, L.*** [1], ***EIRENE, O. A.*** [1]

[1]*Department of Mathematics, Federal University of Petroleum Resources Effurun, Delta State, Nigeria*

ARTICLE INFO

Received: 10/12/2024
Accepted: 02/04/2025

Keywords

Antiretroviral Therapy, ART Adherence, HIV, HIV Prevention, Public Health, Transmission Dynamics, Viral Load Suppression

ABSTRACT

Antiretroviral Therapy (ART) has revolutionized the management of HIV/AIDS, significantly reducing morbidity and mortality rates among infected individuals. This study explores the effects of Antiretroviral Therapy (ART) on the transmission dynamics of HIV, employing a mathematical modeling approach to analyze the interactions between various population compartments. The study demonstrates that ART significantly lowers viral loads to undetectable levels, thereby reducing the risk of HIV transmission. Through sensitivity analysis, we identify key parameters influencing treatment outcomes, particularly highlighting the critical role of ART adherence and initiation rates in shaping community transmission dynamics. The findings emphasize the necessity of addressing barriers to ART access and adherence, especially among vulnerable populations. Furthermore, this work contributes to public health strategies aimed at achieving the UNAIDS 90-90-90 targets by providing insights into the effectiveness of ART as a cornerstone of HIV prevention and treatment programs. Overall, our analysis underscores the importance of continued research and innovation in HIV management to enhance treatment efficacy and improve health outcomes for individuals living with HIV.

1. INTRODUCTION

Human Immunodeficiency Virus (HIV) remains a critical global health issue, with millions affected and new infections occurring daily. Antiretroviral Therapy (ART) has transformed HIV/AIDS from a fatal disease into a manageable chronic condition. This study explores ART's impact on HIV transmission, focusing on viral load suppression, transmission rates, and broader public health implications.

Mathematical models, such as the Susceptible-Infectious-Treated (SIT) model, help simulate disease progression and ART's effects (Cohen et al., 2011). ART suppresses HIV replication, reducing viral loads to undetectable levels. The "Undetectable = Untransmittable" (U=U) principle reflects the inability of individuals with undetectable viral loads to transmit the virus sexually (Smith and Wagner, 2023). ART also reduces morbidity, mortality, and community-level incidence, supporting the treatment-as-prevention (TasP) strategy (Delaney et al., 2022). However, adherence remains critical to maintaining viral suppression (Chang et al., 2023). Pre-Exposure Prophylaxis (PrEP), including long-acting injectable options, has

*Corresponding author, e-mail: okedoye.akindeler@fupre.edu.ng
DIO

proven effective in high-risk populations, though adherence challenges persist, particularly among young women in sub-Saharan Africa (Molina et al., 2022; Grant et al., 2023).

Behavioral and structural interventions also play vital roles. Digital tools and community-based programs promote safer practices and PrEP uptake, emphasizing culturally tailored approaches for groups like men who have sex with men (MSM) (Schnall et al., 2023; Jones et al., 2024). Social determinants such as housing instability and gender-based violence influence transmission, highlighting the need for integrated strategies (Smith et al., 2023; Wilson et al., 2024). The COVID-19 pandemic disrupted HIV services but expanded telehealth opportunities (Kalichman et al., 2023). Promising advances in HIV vaccine research, particularly mRNA-based trials, offer hope (Nguyen et al., 2024).

Key populations, including sex workers and transgender individuals, face ongoing challenges. Legal reforms and harm reduction strategies are essential to improving access (Beyrer et al., 2023; Jin et al., 2022). Despite progress in ART and PrEP, socioeconomic disparities and stigma persist as barriers (Garcia et al., 2024; Johnson et al., 2022). Emerging technologies like artificial intelligence and integrated care for co-infections present opportunities for improved prevention (Zhang et al., 2023; Rodriguez et al., 2022). Continued research and innovation are crucial to addressing HIV across diverse populations.

This study underscores the need for continued research into HIV transmission dynamics. Evolving treatments like ART and PrEP and innovations in digital health require updated approaches to HIV prevention and treatment, particularly across diverse populations affected by social and economic barriers.

2. MATHEMATICAL FORMULATION

The study of the "Effects of Antiretroviral Therapy (ART) on the Transmission Dynamics of HIV" seeks to understand how treatment interventions influence the progression and spread of HIV within a population. In this context, mathematical modeling is a valuable tool, allowing us to capture the complex interplay between infection, treatment, recovery, and progression to AIDS within a population. The model divides the total population into several key compartments: susceptible individuals ($S(t)$), those infected with HIV ($I(t)$), individuals receiving ART ($T(t)$), vaccinated individuals (V (t)), recovered individuals ($R(t)$), and individuals who have progressed to AIDS ($A(t)$). Each compartment has specific dynamics that influence both the spread of HIV and the effectiveness of ART interventions. These compartments interact through several pathways, such as infection from susceptible to infected states, treatment from infected to ART-receiving states, and progression from HIV to AIDS.

The compartmental model that provides a framework for analyzing the transmission dynamics of HIV under the influence of ART is given if Fig. 1 below.

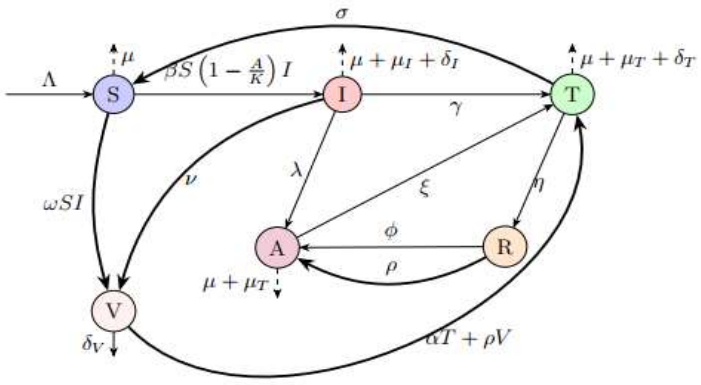

Figure 3.1: Compartmental Diagram for HIV Transmission Dynamics with ART

From the above compartments diagram, the corresponding system of equation for the problem under consideration becomes:

$$\frac{dS(t)}{dt} = \Lambda + \sigma T(t) - \frac{\beta S(t)}{N}\left(1 - \frac{P}{K}\right) I(t) - \omega S(t)\, I(t) - \mu S(t) \quad (1)$$

$$\frac{dI}{dt} = \frac{\beta S(t)}{N}\left(1 - \frac{P}{K}\right) I(t) - \gamma I(t) - (\mu + \mu_I + \delta_I + \nu + \lambda) I(t) \quad (2)$$

$$\frac{dT}{dt} = \gamma I(t) + \xi A(t) + (\alpha - \eta - \mu - \delta_T - \mu_T)\, T(t) + \rho V(t) \quad (3)$$

$$\frac{dV}{dt} = \omega S(t) I(t) + \nu I(t) - \alpha T(t) - (\delta + \rho) V(t) \quad (4)$$

$$\frac{dR}{dt} = \eta T(t) - (\phi + \rho + \mu) R(t) \quad (5)$$

$$\frac{dA}{dt} = \lambda I(t) + (\rho + \phi) R(t) - (\xi + \mu_A + \mu) A(t) \quad (6)$$

Table 1: Parameter definitions and values for HIV transmission model with ART effects

Parameter	Definition	Value	Units
Λ	Recruitment rate into the population	0.01	individuals/day
μ	Natural death rate	0.02	1/year
σ	Rate of ART initiation	0.02	1/day
β	HIV transmission rate	0.01	1(individual day)
N	Total population size	100,000	individuals
K	AIDS population carrying capacity	1000	individuals
ω	HIV-induced immune activation rate	0.12	1/day
γ	Progression rate from infected to treated class	0.1	1/day
μ_I	HIV-induced death rate for infected individuals	0.01	1/day
δ_I	Additional mortality due to HIV	0.005	1/day
ν	Rate of viral rebound	0.01	1/day
λ	Rate of progression to AIDS	0.01	1/day
ξ	Rate of ART effect on AIDS population	0.01	1/day
α	Rate of viral activation in treated class	0.01	1/day

*Corresponding author, e-mail: okedoye.akindeler@fupre.edu.ng
DIO

η	Rate of immune system recovery	0.05	1/day
δ_T	Additional mortality due to ART	0.02	1/day
μ_T	Natural death rate in treated population	0.01	1/year
ρ	Loss rate from recovery to reinfection	0.01	1/day
δ	Rate of viral decay	0.01	1/day
ϕ	Rate of immune activation in recovered class	0.005	1/day
μ_A	Natural death rate in AIDS class	0.05	1/year

The initial data are

$$S(0) = 5{,}000, I(0) = 100, T(0) = 50, V(0) = 5, R(0) = 5, A(0) = 20 \quad (7)$$

3. MODEL ANALYSIS

This study utilizes a mixed-methods approach, combining quantitative with qualitative analysis of epidemiological data. The effectiveness of ART in reducing HIV transmission is analyzed through modeling and comparative analysis of ART coverage and HIV incidence rates across different compartment.

3.1 Positivity of Solutions

For biological models, the state variables represent population subgroups (such as the susceptible population $S(t)$, infected population $I(t)$, etc.). Since populations cannot be negative, it's important to establish that the solutions to the system are non-negative for all $t \geq 0$, given non-negative initial conditions.

Theorem (Positivity of Solutions)

Consider the system of differential equations (1) – (6) subject to (7), governing the dynamics of HIV transmission under ART with initial conditions $S(0) \geq 0, I(0) \geq 0, T(0) \geq 0, V(0) \geq 0, R(0) \geq 0,$ and $A(0) \geq 0$. Then, the solutions $S(t), I(t), T(t), V(t), R(t)$, and $A(t)$ remain non-negative for all $t \geq 0$.

Proof

By assumption, each variable $S(0), I(0), T(0), V(0), R(0), A(0) \geq 0$.

From (1), has a recruitment term Λ and a positive transfer term $\sigma T(t)$. Loss terms are proportional to $S(t)$ itself or $S(t)I(t)$, which implies that as long as $S(0) \geq 0, S(t)$ remains non-negative for $t \geq 0$. Hence,

$$S(t) \geq 0 \; for \; t \geq 0.$$

From equation (2),

$$\frac{dI}{dt} \geq -\gamma I(t) - (\mu + \mu_I + \delta_I + \nu + \lambda)I(t)$$

Which implies

$$\ln I(t) \geq -(\gamma + \mu + \mu_I + \delta_I + \nu + \lambda)t + C$$

That is

$$I(t) \geq L \exp(-(\gamma + \mu + \mu_I + \delta_I + \nu + \lambda)t) \quad (8)$$

where $L = e^C$ is a constant. Since exponential is a non-negative number, it then implies that, $I(t) \geq 0$ for $t \geq 0$.

So also, from equations (3) – (6), following the same procedure we have

$$T(t) \geq L_1 e^{-(\eta + \mu + \delta_T + \mu_T)t}, R(t) \geq L_2 e^{-(\phi + \rho + \mu)t}, A(t) \geq L_3 e^{-(\xi + \mu_A + \mu)t} \quad (9)$$

By equation (4),

$$\frac{dV}{dt} \geq -\alpha T(t) - (\delta + \rho)V(t)$$

that is

$$\frac{dV(t)}{dt} + (\delta + \rho)V(t) \geq -\alpha L_4 e^{(-(\eta + \mu + \delta_T + \mu_T)t)}$$

Such that

$$V(t) \geq \frac{\alpha L_1}{(\eta + \mu + \delta_T + \mu_T) - (\delta + \rho)} e^{(-(\eta + \mu + \delta_T + \mu_T)t)}$$

From equation (8) – (10), each of the differential equations preserves non-negativity given non-negative initial conditions, which means that if $S(0), I(0), T(0), V(0), R(0), A(0) \geq 0$, then $S(t), I(t), T(t), V(t), R(t), A(t) \geq 0$ for all $t \geq 0$.

3.2 Boundedness of Solutions

To ensure biological relevance, we also need to establish that the solutions are bounded, meaning that each population does not grow without bound but instead remains within a reasonable range over time. This is to allows the investigation of the long-term effects of ART on HIV transmission without concerns over unrealistic population behaviors in the model.

Total Population Bound: Let $N(t) = S(t) + I(t) + T(t) + V(t) + R(t) + A(t)$, the total population at time t. Summing all differential equations gives:

$$\frac{dN(t)}{dt} = \Lambda - \mu N(t) - \mu_I I(t) - \mu_T T(t) - \mu_A A(t). \quad (11)$$

Since μ, μ_I, μ_T , and μ_A represent natural death rates, they help limit the growth of $N(t)$, suggesting that $N(t)$ approaches a steady state as $t \to \infty$.

Now, from equations (8) and (9),

$$\frac{dN(t)}{dt} \leq \Lambda - (\mu + \mu_I)L \exp(-(\gamma + \mu + \mu_I + \delta_I + \nu + \lambda)t) - \mu_T L_1 e^{-(\eta + \mu + \delta_T + \mu_T)t} - \mu_A L_3 e^{-(\xi + \mu_A + \mu)t} \quad (10)$$

$$N(t) \leq \Lambda t + \frac{(\mu + \mu_I)L}{\gamma + \mu + \mu_I + \delta_I + \nu + \lambda} x \exp(-(\gamma + \mu + \mu_I + \delta_I + \nu + \lambda)t) + \frac{\mu_A L_3}{\xi + \mu_A + \mu} e^{-(\xi + \mu_A + \mu)t} + \frac{\mu_T L_1}{\eta + \mu + \delta_T + \mu_T} e^{-(\eta + \mu + \delta_T + \mu_T)t} \quad (12)$$

We observe that

$$\exp(-\phi(t)) \leq 1 \; \forall \; t \geq 0, \quad (13)$$

Consequently, $N(t)$ bounded!

3.3 Existence and Uniqueness of Solution

The existence and uniqueness of solutions can be established using classical results from the theory of ODEs, particularly the Picard-Lindelof theorem.

Theorem (Existence and Uniqueness of Solutions)

Let $X(t) = [S(t), I(t), T(t), V(t), R(t), A(t)]^\top$ be a vector-valued function governed by the system of first-order differential equations:

$$\frac{dX}{dt} = F(X(t)), \quad (14)$$

where $F: R^6 \to R^6$ is defined by

$$F(X) = \begin{bmatrix} \Lambda + \sigma T - \frac{\beta S}{N}\left(1 - \frac{P}{K}\right) I - \omega S I - \mu S \\ \frac{\beta S}{N}\left(1 - \frac{P}{K}\right) - \gamma I - (\mu + \mu I + \delta I + \nu + \lambda) I \\ \gamma I + \xi A + (\alpha - \eta - \mu - \delta T - \mu T) T + \rho V \\ \omega S I + \nu I - \alpha T - (\delta + \rho) V \\ \eta T - (\phi + \rho + \mu) R \\ \lambda I + (\rho + \phi) R - (\xi + \mu A + \mu) A \end{bmatrix}. \quad (15)$$

If the initial conditions $X(0) = X0 = [S(0), I(0), T(0), V(0), R(0), A(0)]^\top$ are given, then there exists a unique solution $X(t)$ to this system for $t \geq 0$, provided that $F(X)$ is continuous and satisfies a Lipschitz condition on the domain of interest.

Proof: Let $X(t) = [S(t), I(t), T(t), V(t), R(t), A(t)]^\top$ as the vector of population compartments, and express the system as

$$\frac{dX}{dt} = F(X), \quad (16)$$

where $F(X)$ represents the right-hand side of the system.

Each component function of $F(X)$ involves operations such as addition, subtraction, multiplication, and division by constants or by the population compartments S, I, T, V, R, and A, which are assumed to be non-negative and finite for all t ≥ 0.

Hence, each component of F(X) is continuous on the domain where $X(t)$ is non-negative and bounded. By the continuity of $F(X)$ on this domain, it satisfies the first condition of the Picard-Lindelof theorem for existence of solutions.

Now, to ensure the uniqueness of solutions, we must verify that $F(X)$ satisfies the Lipschitz condition: there exists a constant $L > 0$ such that, for any two points $X_1, X_2 \in R^6$,

$$\| F(X_1) - F(X_2) \| \leq L \| X_1 - X_2 \|. \quad (17)$$

Since each component of $F(X)$ is either linear or bilinear in terms of S, I, T, V, R, and A, the function differences $|F_i(X_1) - F_i(X_2)|$ are bounded by $|X_{j,1} - X_{j,2}|$ for each variable X_j in X, up to a constant. Therefore, the system satisfies the Lipschitz condition with respect to X in this domain with a Lipschitz constant L.

Since $F(X)$ is both continuous and satisfies the Lipschitz condition on the domain of interest, we can apply the Picard-Lindelof Existence and Uniqueness Theorem, which guarantees that there exists a unique solution $X(t) = [S(t), I(t), T(t), V(t), R(t), A(t)]^\top$ to the initial value problem

$$\frac{dX}{dt} = F(X(t)), X(0) = X_0, \quad (18)$$

for $t \geq 0$.

The continuity of $F(X)$ and the Lipschitz condition on the system ensure that there exists a unique solution $X(t)$ to the differential equations, starting from the initial condition $X(0) = X_0$. Thus, the existence and uniqueness of solutions for the system is established.

3.*4 Equilibrium Points:* To find the equilibrium points of the system modeling the effects of Antiretroviral Therapy (ART) on HIV transmission, we set the time derivatives of each of equations (1) – (6) to zero. This gives us the following system of algebraic equations:

$$\Lambda + \sigma T(t) - \frac{\beta S(t)}{N}\left(1 - \frac{P}{K}\right) I(t) - \omega S(t) I(t) - \mu S(t) = 0 \quad (19)$$

$$\frac{\beta S(t)}{N}\left(1 - \frac{P}{K}\right) I(t) - \gamma I(t) - (\mu + \mu_I + \delta_I + \nu + \lambda) I(t) = 0 \quad (20)$$

$$\gamma I(t) + \xi A(t) + (\alpha - \eta - \mu - \delta_T - \mu_T) T(t) + \rho V(t) = 0 \quad (21)$$

$$\omega S(t) I(t) + \nu I(t) - \alpha T(t) - (\delta + \rho) V(t) = 0 \quad (22)$$

$$\eta T(t) - (\phi + \rho + \mu) R(t) = 0 \quad (23)$$

$$\lambda I(t) + (\rho + \phi) R(t) - (\xi + \mu_A + \mu) A(t) = 0 \quad (24)$$

Assuming, $I(t) \neq 0$, from (20)

$$\left(\frac{\beta S(t)}{N}\left(1 - \frac{P}{K}\right) - \gamma - (\mu + \mu_I + \delta_I + \nu + \lambda)\right) I(t) \quad (25)$$

*Corresponding author, e-mail: okedoye.akindeler@fupre.edu.ng
DIO

Equation (25) imply

$$\begin{pmatrix} S(t) = \dfrac{(\gamma + \mu + \mu_I + \delta_I + \nu + \lambda)}{\dfrac{\beta}{N}\left(1 - \dfrac{P}{K}\right)} & \text{or} \\ I(t) = 0 \end{pmatrix} \tag{26}$$

3.4.1 Disease Free Equilibrium (DFEP)

When $I(t) = 0$, we have Disease Free Equilibrium. solving the system of equations (19) – (23), gives

$$S(t) = \frac{\Lambda}{\mu}, I(t) = 0, T(t) = 0, V(t) = 0, R(t) = 0, A(t) = 0$$

3.4.1 Endemic Equilibrium Point (EEP)

Assuming $I(t) \neq 0$, solving equations (19) – (23) gives:

$$S(t) = \frac{\gamma + e_1}{M},$$

$$I(t) = \frac{\begin{pmatrix} \xi\eta\rho^2 + \begin{pmatrix} -e_2e_3e_4 \\ +\xi\eta(\phi + \delta) \end{pmatrix}\rho \\ +\delta(\phi\xi\eta - e_3e_4(e_2 - \alpha)) \end{pmatrix}(M\Lambda - \mu(\gamma + e_1))}{\xi\eta(\gamma + e_1)(M + \omega)\rho^2},$$

$$\begin{pmatrix} + \left(\begin{pmatrix} M\sigma\lambda\xi + e_4\begin{pmatrix} \begin{pmatrix} (\sigma - e_2)\gamma \\ +\sigma\nu - e_2e_1 \end{pmatrix}M \\ +\omega(\gamma + e_1)(\sigma - e_2) \end{pmatrix} \end{pmatrix}e_3 \right)\rho \\ +\xi\eta(\gamma + e_1)(\phi + \delta)(M + \omega) \\ + \delta\left(\begin{pmatrix} M\sigma\lambda\xi + \begin{pmatrix} \begin{pmatrix} (\sigma - e_2 + \alpha)\gamma \\ -e_1(e_2 - \alpha) \end{pmatrix}M \\ -\omega(e_2 - \alpha)(\gamma + e_1) \end{pmatrix}e_4 \end{pmatrix}e_3 \right) \\ +\phi\xi\eta(\gamma + e_1)(M + \omega) \end{pmatrix},$$

$$T(t) = \frac{e_3\begin{pmatrix} \begin{pmatrix} (\nu + \gamma)e_4 + \lambda\xi \end{pmatrix}\rho \\ +\delta(\gamma e_4 + \lambda\xi) \end{pmatrix}M \\ +\omega e_4\rho(\gamma + e_1) \end{pmatrix}(\mu(\gamma + e_1) - M\Lambda)}{\begin{pmatrix} M\begin{pmatrix} \begin{pmatrix} \xi\eta(\gamma + e_1)\rho^2 + \begin{pmatrix} e_3\begin{pmatrix} (\sigma - e_2)\gamma \\ +\sigma\nu - e_2e_1 \end{pmatrix}e_4 \\ +\begin{pmatrix} \eta(\phi + \delta)\gamma + \sigma\lambda e_3 \\ +\phi\eta e_1 + e_1\eta\delta \end{pmatrix}\xi \end{pmatrix}\rho \\ +\delta\begin{pmatrix} e_3\big((\sigma - e_2 + \alpha)\gamma - e_1(e_2 - \alpha)\big)e_4 \\ +\xi(\eta\gamma\phi + \eta\phi e_1 + \lambda\sigma e_3) \end{pmatrix} \end{pmatrix}M \\ +\omega(\gamma + e_1)\begin{pmatrix} \xi\eta\rho^2 + \begin{pmatrix} e_3(\sigma - e_2)e_4 \\ +\xi\eta(\phi + \delta) \end{pmatrix}\rho \\ +\delta(\phi\xi\eta - e_3e_4(e_2 - \alpha)) \end{pmatrix} \end{pmatrix} \end{pmatrix}},$$

$$V(t) = \frac{\begin{pmatrix}\begin{pmatrix}\begin{pmatrix}(\lambda\xi\alpha - (-\alpha\gamma + \nu(e_2 - \alpha))e_4)M \\ -\omega e_4(e_2 - \alpha)(\gamma + e_1)\end{pmatrix}e_3 \\ +(M\nu + \omega(\gamma + e_1))\eta\xi(\phi + \rho)\end{pmatrix}(M\Lambda - \mu(\gamma + e_1))\end{pmatrix}}{\begin{pmatrix}M\begin{pmatrix}\begin{pmatrix}\begin{pmatrix}\sigma\lambda(\delta + \rho)\xi + e_4\begin{pmatrix}((\sigma - e_2)\gamma + \sigma\nu - e_2e_1)\rho \\ +\delta\begin{pmatrix}(\sigma - e_2 + \alpha)\gamma \\ -e_1(e_2 - \alpha)\end{pmatrix}\end{pmatrix}\end{pmatrix}M \\ +((\sigma - e_2)\rho - \delta(e_2 - \alpha))\omega e_4(\gamma + e_1)\end{pmatrix}e_3 \\ +\xi\eta(\delta + \rho)(\gamma + e_1)(\phi + \rho)(M + \omega)\end{pmatrix}\end{pmatrix}}$$

$$R(t) = \frac{\eta\begin{pmatrix}\begin{pmatrix}((\nu + \gamma)e_4 + \lambda\xi)\rho \\ +\delta(\gamma e_4 + \lambda\xi)\end{pmatrix}M \\ +\omega e_4\rho(\gamma + e_1)\end{pmatrix}(\mu(\gamma + e_1) - M\Lambda)}{\begin{pmatrix}M\begin{pmatrix}\begin{pmatrix}\xi\eta(\gamma + e_1)\rho^2 + \begin{pmatrix}e_3((\sigma - e_2)\gamma + \sigma\nu - e_2e_1)e_4 \\ +\begin{pmatrix}\eta(\phi + \delta)\gamma + \sigma\lambda e_3 \\ +\phi\eta e_1 + e_1\eta\delta\end{pmatrix}\xi\end{pmatrix}\rho \\ +\delta\begin{pmatrix}e_3((\sigma - e_2 + \alpha)\gamma - e_1(e_2 - \alpha))e_4 \\ +\xi(\eta\gamma\phi + \eta\phi e_1 + \lambda\sigma e_3)\end{pmatrix}\end{pmatrix}M \\ +\omega(\gamma + e_1)\begin{pmatrix}\xi\eta\rho^2 + \begin{pmatrix}e_3(\sigma - e_2)e_4 \\ +\xi\eta(\phi + \delta)\end{pmatrix}\rho \\ +\delta(\phi\xi\eta - e_3e_4(e_2 - \alpha))\end{pmatrix}\end{pmatrix}\end{pmatrix}}$$

$$A(t) = \frac{\begin{pmatrix}\begin{pmatrix}\begin{pmatrix}\eta(\nu + \gamma)\rho^2 \\ +\begin{pmatrix}((\phi + \delta)\gamma + \phi\nu)\eta \\ +\lambda e_2e_3\end{pmatrix}\rho\end{pmatrix}M \\ +(\eta\gamma\phi + \lambda e_3(e_2 - \alpha))\delta\end{pmatrix}(\mu(\gamma + e_1) - M\Lambda) \\ +\omega\eta\rho(\gamma + e_1)(\phi + \rho)\end{pmatrix}}{\begin{pmatrix}M\begin{pmatrix}\begin{pmatrix}\xi\eta(\gamma + e_1)\rho^2 + \begin{pmatrix}\xi(\gamma + e_1)(\phi + \delta)\eta \\ +e_3\begin{pmatrix}e_4(\sigma - e_2)\gamma - e_2e_4e_1 \\ +\sigma(\lambda\xi + \nu e_4)\end{pmatrix}\end{pmatrix}\rho \\ +\delta\begin{pmatrix}\phi\xi(\gamma + e_1)\eta \\ +e_3\begin{pmatrix}e_4(\sigma - e_2 + \alpha)\gamma \\ -e_4(e_2 - \alpha)e_1 + \sigma\lambda\xi\end{pmatrix}\end{pmatrix}\end{pmatrix}M \\ +\omega(\gamma + e_1)\begin{pmatrix}\xi\eta\rho^2 + \begin{pmatrix}e_3(\sigma - e_2)e_4 \\ +\xi\eta(\phi + \delta)\end{pmatrix}\rho \\ +\delta(\phi\xi\eta - e_3e_4(e_2 - \alpha))\end{pmatrix}\end{pmatrix}\end{pmatrix}}$$

3.5 Reproduction Number:

In order to find the Basic Reproduction Number, we split the model equations into:

- New Infection Terms (F): These terms account for new infections that arise in the infected compartments.

- Transition Terms ($\mathcal{V}$): These terms represent the flow out of infected compartments, not due to new infections but due to recovery, death, or other transitions.

In this model, the infected compartments are primarily the *I* compartment.

From the system, these terms are:

$$F = \frac{\beta S}{N}\left(\mathbf{1} - \frac{P}{K}\right) I + \omega SI.$$

$$\mathcal{V} = \gamma I + (\mu + \mu I + \delta I + \nu + \lambda)I.$$

The next-generation matrix K is constructed using the partial derivatives of F and $\mathcal{V}$ with respect to I, evaluated at the DFEP. Specifically:

- Partial Derivative of *F* with respect to *I* at DFEP:

$$\left.\frac{\partial F}{\partial I}\right|_{DFEP} = \frac{\beta \frac{\Lambda}{\mu}}{N}\left(1 - \frac{P}{K}\right) + \omega \frac{\Lambda}{\mu}.$$

- Partial Derivative of $\mathcal{V}$ with respect to *I* at DFEP:

$$\left.\frac{\partial \mathcal{V}}{\partial I}\right|_{DFEP} = \gamma + \mu + \mu I + \delta I + \nu + \lambda.$$

Thus, the next-generation matrix *K* for this model is:

$$K = \left.\frac{\partial F}{\partial I}\right|_{DFEP} \times \left(\left.\frac{\partial \mathcal{V}}{\partial I}\right|_{DFEP}\right)^{-1}.$$

Substitute the values:

$$K = \frac{\frac{\beta \frac{\Lambda}{\mu}}{N}\left(1 - \frac{P}{K}\right) + \omega \frac{\Lambda}{\mu}}{\gamma + \mu + \mu_I + \delta_I + \nu + \lambda}.$$

The Basic Reproduction Number R_0 is the spectral radius (dominant eigenvalue) of the next generation matrix K. Since K is a scalar here, R_0 is simply the value of K:

$$\frac{\frac{\beta \frac{\Lambda}{\mu}}{N}\left(1 - \frac{P}{K}\right) + \omega \frac{\Lambda}{\mu}}{\gamma + \mu + \mu_I + \delta_I + \nu + \lambda}.$$

Effective Reproduction Number, Re

The Effective Reproduction Number Re takes into account the current state of the population, especially the proportion of susceptible individuals. Therefore, Re depends on both $R0$ and the current susceptible population *S*.

$$Re = R_0 \cdot \frac{S}{N}.$$

Substituting *S* from the endemic equilibrium point:

$$Re = \frac{\left(\frac{\beta}{N}\left(1 - \frac{P}{K}\right) + \omega\right)\frac{\Lambda}{\mu}}{\beta\left(1 - \frac{P}{K}\right)}$$

3.6 Stability Analysis

The model can be analyzed for stability and equilibrium points to understand the long-term behavior of the epidemic. To analyze the stability of the system describing the effects of Antiretroviral Therapy (ART) on the transmission dynamics of HIV, we typically perform stability analysis on two key equilibrium points:

The Jacobian matrix *J* at the equilibrium point is defined as follows:

$$J = \begin{bmatrix} -(M+\omega)I(t) - \mu & -(M+\omega)I(t) & \sigma & 0 & 0 & 0 \\ ItM & MS(t) - \gamma - e_1 & 0 & 0 & 0 & 0 \\ 0 & \gamma & \alpha - e_2 & \rho & 0 & \xi \\ \omega I & S(t)\,\omega + \nu & -\alpha & -\delta - \rho & 0 & 0 \\ 0 & 0 & \eta & 0 & -e_3 & 0 \\ 0 & \lambda & 0 & 0 & \varphi + \rho & -e_4 \end{bmatrix} \quad (27)$$

1. Disease-Free Equilibrium Point (DFEP): The DFEP is given by:

$$(\boldsymbol{S},\boldsymbol{I},\boldsymbol{T},\boldsymbol{V},\boldsymbol{R},\boldsymbol{A}) = \left(\frac{\Lambda}{\mu},0,0,0,0,0\right).$$

Simplified Jacobian at DFEP: Now simplifying, we find:

$$\boldsymbol{J}_{DFEP} = \begin{bmatrix} -\mu & -\frac{M\Lambda}{\mu} - \frac{\omega\Lambda}{\mu} & \sigma & 0 & 0 & 0 \\ 0 & \frac{M\Lambda}{\mu} - \gamma - e_1 & 0 & 0 & 0 & 0 \\ 0 & \gamma & \alpha - e_2 & \rho & 0 & \xi \\ 0 & \frac{\omega\Lambda}{\mu} + \nu & -\alpha & -\delta - \rho & 0 & 0 \\ 0 & 0 & \eta & 0 & -e_3 & 0 \\ 0 & \lambda & 0 & 0 & \varphi + \rho & -e_4 \end{bmatrix} \quad (28)$$

where $e_1 = \mu + \mu_I + \boldsymbol{\delta}_I + \boldsymbol{\nu} + \boldsymbol{\lambda_1}, e_2 = \eta + \mu + \delta_T + \mu_T, e_3 = \phi + \rho + \mu, e_4 = \xi + \mu_A + \mu$

Since the matrix is block diagonal, we can analyze the blocks separately.

The characteristics polynomial is given by

$$64\Omega^6 + (32\mu - 32a_2 - 32a_3 - 32a_5 + 32e_3 + 32e_4)\Omega^5 + (16\alpha\rho - 16\mu a_2 - 16\mu a_3 - 16\mu a_5$$

$$+16\mu e_3 + 16\mu e_4 + 16a_2a_3 + 16a_2a_5 - 16a_2e_3 - 16a_2e_4 + 16a_3a_5 - 16a_3e_3 - 16a_3e_4$$

$$- 16a_5e_3 - 16a_5e_4 + 16e_3e_4)\Omega^4 + (8\alpha\rho\mu - 8\alpha\rho a_2 + 8\alpha\rho e_3 + 8\alpha\rho e_4 - 8\eta\xi a_6 + 8\mu a_2a_3$$

$$+ 8\mu a_2a_5 - 8\mu a_2e_3 - 8\mu a_2e_4 + 8\mu a_3a_5 - 8\mu a_3e_3 - 8\mu a_3e_4 - 8\mu a_5e_3 - 8\mu a_5e_4 + 8\mu e_3e_4$$

$$- 8a_2a_3a_5 + 8a_2a_3e_3 + 8a_2a_3e_4 + 8a_2a_5e_3 + 8a_2a_5e_4 - 8a_2e_3e_4 + 8a_3a_5e_3 + 8a_3a_5e_4$$

$$- 8a_3e_3e_4 - 8a_5e_3e_4)\Omega^3 + (-4\alpha\rho\mu a_2 + 4\alpha\rho\mu e_3 + 4\alpha\rho\mu e_4 - 4\alpha\rho a_2e_3 - 4\alpha\rho a_2e_4$$

$$+4\alpha\rho e_3e_4 - 4\eta\xi\mu a_6 + 4\eta\xi a_2a_6 + 4\eta\xi a_5a_6 - 4\mu a_2a_3a_5 + 4\mu a_2a_3e_3 + 4\mu a_2a_3e_4$$

$$+ 4\mu a_2a_5e_3 + 4\mu a_2a_5e_4 - 4\mu a_2e_3e_4 + 4\mu a_3a_5e_3 + 4\mu a_3a_5e_4 - 4\mu a_3e_3e_4 - 4\mu a_5e_3e_4$$

$$- 4a_2a_3a_5e_3 - 4a_2a_3a_5e_4 + 4a_2a_3e_3e_4 + 4a_2a_5e_3e_4 + 4a_3a_5e_3e_4)\Omega^2 + (-2\alpha\rho\mu a_2e_3$$

$$- 2\alpha\rho\mu a_2e_4 + 2\alpha\rho\mu e_3e_4 - 2\alpha\rho a_2e_3e_4 + 2\eta\xi\mu a_2a_6 + 2\eta\xi\mu a_5a_6 - 2\eta\xi a_2a_5a_6$$

$$- 2\mu a_2a_3a_5e_3 - 2\mu a_2a_3a_5e_4 + 2\mu a_2a_3e_3e_4 + 2\mu a_2a_5e_3e_4 + 2\mu a_3a_5e_3e_4 - 2a_2a_3a_5e_3e_4)\Omega$$

$$-\alpha\rho\mu a_2e_3e_4 - \eta\xi\mu a_2a_5a_6 - \mu a_2a_3a_5e_3e_4.$$

The above characteristic polynomial equation is of the form

$$P(\Omega) = c_6\Omega^6 + c_5\Omega^5 + c_4\Omega^4 + c_3\Omega^3 + c_2\Omega^2 + c_1\Omega + c_0 = 0$$

$c_6 = 64,$

$c_5 = 32\mu - 32a_2 - 32a_3 - 32a_5 + 32e_3 + 32e_4,$

$c_4 = 16\alpha\rho - 16\mu a_2 - 16\mu a_3 - 16\mu a_5 + 16\mu e_3 + 16\mu e_4 + 16a_2a_3 + 16a_2a_5 - 16a_2e_3$
$- 16a_2e_4 + 16a_3a_5 - 16a_3e_3 - 16a_3e_4 - 16a_5e_3 - 16a_5e_4 + 16e_3e_4,$

$$c_3 = 8\alpha\rho\mu - 8\alpha\rho a_2 + 8\alpha\rho e_3 + 8\alpha\rho e_4 - 8\eta\xi a_6 + 8\mu a_2 a_3 + 8\mu a_2 a_5 - 8\mu a_2 e_3 - 8\mu a_2 e_4 + 8\mu a_3 a_5 - 8\mu a_3 e_3 - 8\mu a_3 e_4 - 8\mu a_5 e_3 - 8\mu a_5 e_4 + 8\mu e_3 e_4 - 8a_2 a_3 a_5 + 8a_2 a_3 e_3 + 8a_2 a_3 e_4 + 8a_2 a_5 e_3 + 8a_2 a_5 e_4 - 8a_2 e_3 e_4 + 8a_3 a_5 e_3 + 8a_3 a_5 e_4 - 8a_3 e_3 e_4 - 8a_5 e_3 e_4,$$

$$c_2 = -4\alpha\rho\mu a_2 + 4\alpha\rho\mu e_3 + 4\alpha\rho\mu e_4 - 4\alpha\rho a_2 e_3 - 4\alpha\rho a_2 e_4 + 4\alpha\rho e_3 e_4 - 4\eta\xi\mu a_6 + 4\eta\xi a_2 a_6 + 4\eta\xi a_5 a_6 - 4\mu a_2 a_3 a_5 + 4\mu a_2 a_3 e_3 + 4\mu a_2 a_3 e_4 + 4\mu a_2 a_5 e_3 + 4\mu a_2 a_5 e_4 - 4\mu a_2 e_3 e_4 + 4\mu a_3 a_5 e_3 + 4\mu a_3 a_5 e_4 - 4\mu a_3 e_3 e_4 - 4\mu a_5 e_3 e_4 - 4a_2 a_3 a_5 e_3 - 4a_2 a_3 a_5 e_4 + 4a_2 a_3 e_3 e_4 + 4a_2 a_5 e_3 e_4 + 4a_3 a_5 e_3 e_4,$$

$$c_1 = -2\alpha\rho\mu a_2 e_3 - 2\alpha\rho\mu a_2 e_4 + 2\alpha\rho\mu e_3 e_4 - 2\alpha\rho a_2 e_3 e_4 + 2\eta\xi\mu a_2 a_6 + 2\eta\xi\mu a_5 a_6 - 2\eta\xi a_2 a_5 a_6 - 2\mu a_2 a_3 a_5 e_3 - 2\mu a_2 a_3 a_5 e_4 + 2\mu a_2 a_3 e_3 e_4 + 2\mu a_2 a_5 e_3 e_4 + 2\mu a_3 a_5 e_3 e_4 - 2a_2 a_3 a_5 e_3 e_4$$

$$c_0 = -\alpha\rho\mu a_2 e_3 e_4 - \eta\xi\mu a_2 a_5 a_6 - \mu a_2 a_3 a_5 e_3 e_4.$$

By Routh-Hurwitz criterion governing the polynomials of order 6 the system is stable if all and only if all roots of the equation have negative real parts. And for the system to be stable, all entries in the first column of the Routh array must be positive.

1. $c_6 > 0$
2. $c_5 > 0$
3. $b_{31} > 0$
4. $b_{41} > 0$
5. $b_{51} > c_3$

where $b_{31} = \frac{c_4 c_5 - 32 c_3}{c_6}, b_{41} = \frac{b_{31} c_5 - c_6 b_{32}}{b_{31}}, b_{51} = \frac{b_{41}\, b_{32} - b_{31} b_{42}}{b_{41}}, b_{32} = \frac{c_4 c_6 - 32 c_2}{c_4}, b_{42} = \frac{b_{31} c_6}{b_{31}}$

From the expansion above, all the conditions are satisfied. Therefore, the disease-free equilibrium is locally asymptotically stable. This completes the proof.

Sensitivity Analysis

The sensitivity S_x of R_0 with respect to a parameter *x* can be defined as:

$$S_x = \frac{\partial R_0}{\partial x} \cdot \frac{x}{R_0}$$

The model parameters: $\Lambda, \mu, \beta, N, P, K, \omega, \gamma, \mu_I, \delta_I, \nu$, and λ are obtained as follows:

$$S_\Lambda = \frac{1}{\mu}\left(\frac{\beta}{N}\left(1 - \frac{P}{K}\right) + \omega\right) \cdot \frac{\Lambda}{R_0(\gamma + \mu + \mu i + \delta i + \nu + \lambda)}$$

$$S_\mu = -\frac{\Lambda\left(\frac{\beta}{N}\left(1 - \frac{P}{K}\right) + \omega\right)}{\mu^2(\gamma + \mu + \mu i + \delta i + \nu + \lambda)} \cdot \frac{\mu}{R_0}$$

$$S_\beta = \frac{\Lambda}{\mu} \cdot \frac{1}{N}\left(1 - \frac{P}{K}\right) \cdot \frac{1}{R_0(\gamma + \mu + \mu i + \delta i + \nu + \lambda)} \cdot \beta$$

$$S_N = -\frac{\Lambda}{\mu}\frac{\beta}{N^2}\left(1 - \frac{P}{K}\right)\cdot\frac{N}{R_0(\gamma+\mu+\mu_i+\delta_i+\nu+\lambda)}$$

$$S_P = \frac{\Lambda}{\mu}\frac{\beta}{NK}\cdot\frac{P}{R_0(\gamma+\mu+\mu_i+\delta_i+\nu+\lambda)}$$

$$S_K = -\frac{\Lambda}{\mu}\frac{\beta}{NK^2}\cdot\frac{K}{R_0(\gamma+\mu+\mu_i+\delta_i+\nu+\lambda)}$$

$$S_\omega = \frac{\frac{\Lambda}{\mu}\omega}{R_0(\gamma+\mu+\mu_i+\delta_i+\nu+\lambda)}, S_\gamma = \frac{-\frac{\Lambda}{\mu}\left(\frac{\beta}{N}\left(1-\frac{P}{K}\right)+\omega\right)\gamma}{R_0(\gamma+\mu+\mu_i+\delta_i+\nu+\lambda)^2}$$

$$S_{\mu_i} = \frac{-\frac{\Lambda}{\mu}\left(\frac{\beta}{N}\left(1-\frac{P}{K}\right)+\omega\right)\mu_i}{R_0(\gamma+\mu+\mu i+\delta i+\nu+\lambda)^2}, S_{\delta_i} = \frac{-\frac{\Lambda}{\mu}\left(\frac{\beta}{N}\left(1-\frac{P}{K}\right)+\omega\right)\delta_i}{R_0(\gamma+\mu+\mu_i+\delta_i+\nu+\lambda)^2}$$

$$S_\nu = \frac{-\frac{\Lambda}{\mu}\left(\frac{\beta}{N}\left(1-\frac{P}{K}\right)+\omega\right)\nu}{R_0(\gamma+\mu+\mu_i+\delta_i+\nu+\lambda)^2}, S_\lambda = \frac{-\frac{\Lambda}{\mu}\left(\frac{\beta}{N}\left(1-\frac{P}{K}\right)+\omega\right)\lambda}{R_0(\gamma+\mu+\mu_i+\delta_i+\nu+\lambda)^2}$$

Table 2: Sensitivity indices with the base values in Table 1 ($R_0 = 0.21$)

Parameter	Index		Parameter	Index
S_Λ	1.0000000000		S_{δ_i}	-0.0172413793
S_ω	0.9999999174		S_λ	-0.0344827586
S_β	0.0000000825		S_{μ_i}	-0.0483132028
S_P	0.0000000083		S_γ	-0.3448275862
S_N	-0.0000000001		S_ν	-0.3448275862
S_K	-0.0000009864		S_μ	-1.0000000000

4. NUMERICAL SIMULATION

The numerical solution of this model employs Maple to simulate and analyze ART's impact through numerical simulations and graphical outputs. Maple's advanced computational tools enable precise scenario simulations and trend visualization, enhancing data interpretation. Numerical simulations are performed to study the impact of various parameters, on the transmission dynamics of HIV.

Figures 4.1 and 4.2 demonstrate the effects of recruitment rates (Λ) on the dynamics of susceptible and vaccinated populations over time, measured in weeks. Figure 4.1 shows the impact of varying Λ on the number of susceptible individuals (S(t)). A higher recruitment rate significantly increases the susceptible population. For example, when Λ=0.9 (dashed black line), the susceptible population grows rapidly compared to Λ=0.3 (red line) or Λ=0 (solid black line). With positive Λ, the susceptible population grows consistently over time, whereas it declines when Λ=0, reflecting the absence of new individuals entering the population. This suggests that high recruitment rates expand the pool of individuals at risk of HIV, emphasizing the need for targeted interventions, such as vaccination or educational programs, to mitigate transmission. Figure 4.2 illustrates the vaccinated population over time for different Λ values. As Λ increases, the initial peak of

vaccinated individuals rises but declines more rapidly afterward. For Λ=0 (solid black line), the vaccinated population achieves the highest initial peak around week 1 and decreases gradually. Conversely, with Λ=0.9 (dashed black line), the decline occurs faster, likely due to new susceptible individuals diluting the vaccinated group.

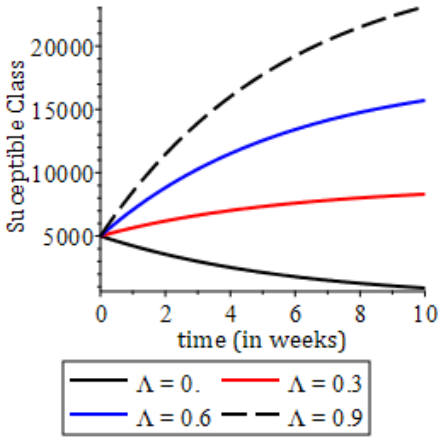

Figure 5.1: Effect of recruitment rate on the susceptible class

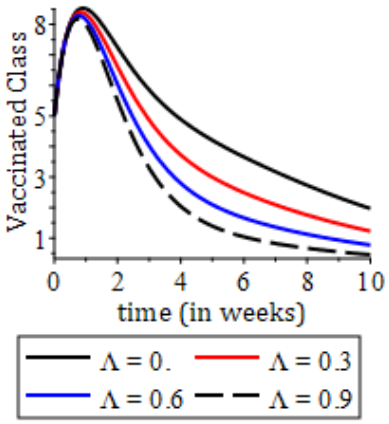

Figure 4.2: Effect of recruitment rate on the vaccinated class

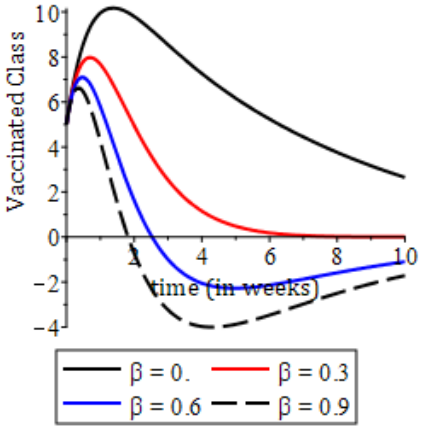

Figure 4.3: Effect of transmission rate on the vaccinated class

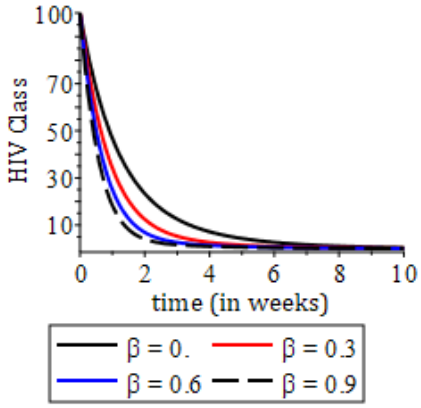

Figure 4.4: Effect of transmission rate on the infected (HIV) class

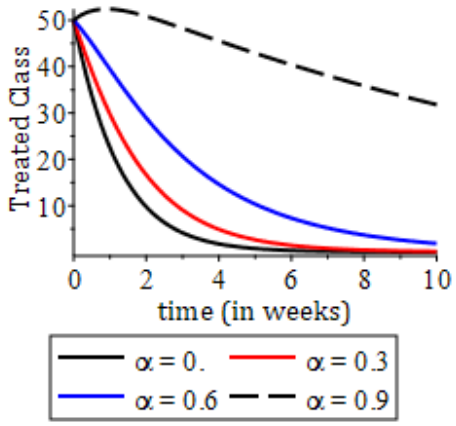

Figure 4.5: Effect of viral activation on treated class

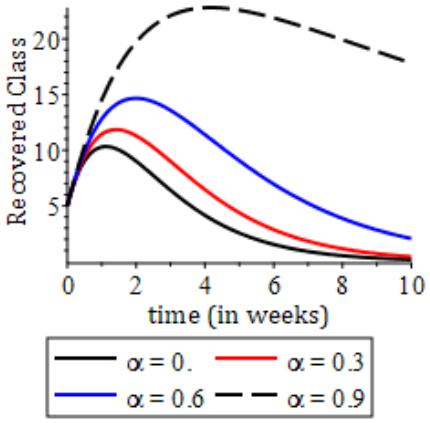

Figure 4.6: Effect of viral activation on recovered class

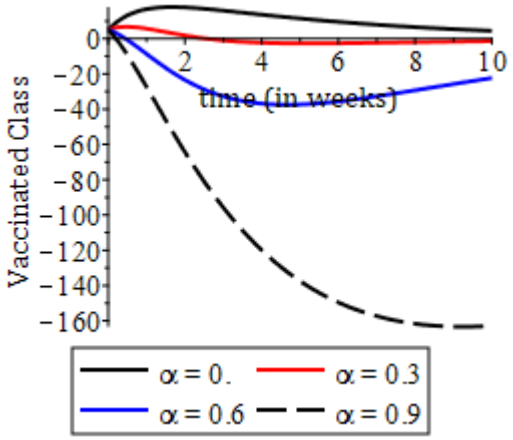

Figure 4.7: Effect of viral activation on vaccinated class

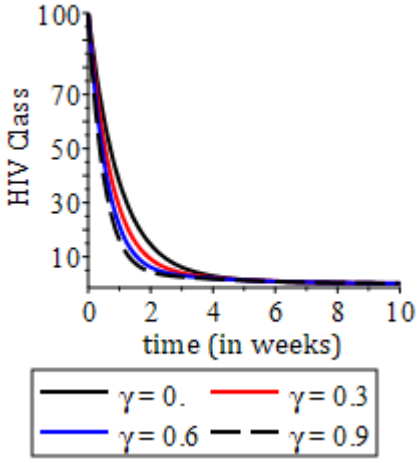

Figure 4.8: Effect of progression rate from infected to treated class on infected (HIV) class

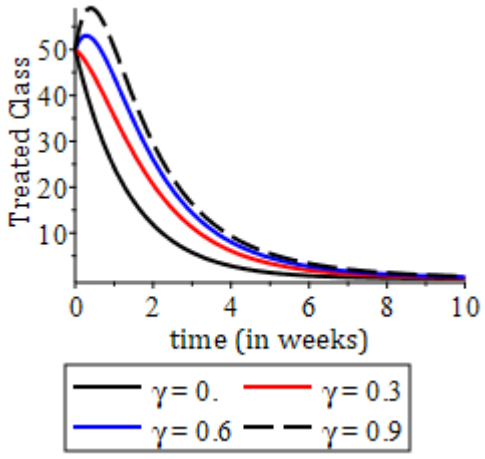

Figure 4.9: Effect of progression rate from infected to treated class on treated class

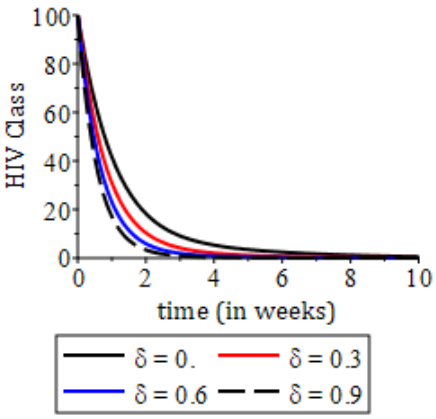

Figure 4.10: Effect of viral decay on the infected (HIV) class

This underscores the importance of sustained vaccination efforts in populations with high recruitment rates to maintain immunity and control HIV transmission.

Figures 4.3 and 4.4 illustrate the dynamics of vaccinated and infected populations under varying HIV transmission rates (β) over time (in weeks), revealing critical insights into transmission dynamics. In Figure 4.3, the vaccinated population exhibits differing trends based on β values. At high transmission rates, such as $\beta = 0.9$ (dashed black line), the vaccinated population peaks early but declines sharply, even becoming negative by week 4, potentially indicating a model artifact or rapid depletion of the vaccinated compartment. Lower transmission rates, such as $\beta = 0.3$ (red line) or $\beta = 0$ (solid black line), result in more stable vaccinated populations, with slower declines over time. The stability at $\beta = 0$ emphasizes minimal pressure on the vaccinated compartment, whereas high transmission rates suggest a need for supplemental interventions like ART to sustain immunity levels. This highlights the challenge of relying solely on vaccination in high-transmission settings. Figure 4.4 shows the infected population's response to varying β values. At $\beta = 0$, the infected population remains relatively stable with minimal decline. However, as β increases (e.g., $\beta = 0.9$), the infected population decreases significantly, suggesting faster transitions out of the infected compartment. These transitions may result from increased progression to AIDS, ART initiation, or higher mortality rates associated with high transmission. This emphasizes β's dual role in driving infections while accelerating infected population depletion through disease progression and mortality.

In Figure 4.5, depicting the treated class, an increase in the viral activation rate (α) from 0 to 0.9 correlates with a gradual rise in the treated population, culminating in a sharp increase at $\alpha = 0.9$. This suggests that higher α values enhance viral reactivation, retaining more individuals in the treated class rather than allowing progression to recovery or AIDS. The sharp rise at $\alpha = 0.9$ may indicate a threshold effect, where reactivation becomes significantly more frequent. Similarly, Figure 4.6 shows a comparable trend in the recovered class. As α increases, more individuals transition into the recovered compartment, likely due to immune responses triggered by reactivation. At $\alpha = 0.9$, a sharp rise occurs, mirroring the treated class's behavior. This suggests that while moderate α values stimulate immune recovery, very high α values cause a pronounced influx into recovery.

In contrast, Figure 4.7 shows that increasing α drives the vaccinated population into the negative region. This decline likely reflects a depletion effect, where reactivation diminishes vaccination effectiveness, potentially due to reinfection risks. Negative values may indicate a theoretical artifact, signifying vaccination's inability to counteract reactivation-driven infections under high α scenarios. The viral activation rate α significantly impacts all compartments, emphasizing its importance in HIV management strategies. As γ increases from 0 to 0.9, figures 4.8 and 4.9 illustrate significant trends in the infected (I(t)) and treated (T(t)) classes, reflecting ART's impact. In the infected class, a gradual reduction occurs as γ rises, indicating that more individuals transition from infection to treatment. This aligns with γ's role as the progression rate to ART, showcasing how scaling up ART reduces untreated infections and the burden of HIV. Conversely, the treated class expands with increasing γ, reflecting the broader reach and effectiveness of ART in managing HIV and reducing transmission through viral load suppression.
Additionally, figure 4.10 demonstrates the effects of δ (viral decay rate). As δ increases,

*Corresponding author, e-mail: okedoye.akindeler@fupre.edu.ng
DIO

the infected class size declines, consistent with faster viral suppression outcomes. A higher δ accelerates viral clearance in infected individuals, reducing viral loads and lowering HIV transmissibility. This results in fewer new infections and a gradual reduction in the infected population. The combination of higher γ and δ highlights the synergistic effects of ART uptake and viral suppression strategies in reducing HIV spread. These trends underscore ART's dual role in transitioning individuals to treatment and curbing transmission by effectively managing viral loads and preventing disease progression.

5. SENSITIVITY INDICES AND ITS IMPLICATION(S) ON THE MODEL

The sensitivity analysis highlights the impact of various parameters on the basic reproduction number (R_0) in HIV transmission dynamics. The recruitment rate (Λ) has a sensitivity index of 1, indicating that population influx increases R_0 by adding susceptible individuals. Targeted screening, HIV awareness, and testing in high-influx areas could help manage this effect. Conversely, the natural death rate (μ) has a sensitivity index of -1, reducing R_0 by lowering the susceptible population. While not directly controllable, improving general healthcare can maintain population health without inadvertently increasing transmission.

The HIV-induced immune activation rate (ω), with a sensitivity index near 1, significantly raises R_0. Early ART initiation can stabilize the immune system, delaying activation and slowing disease progression. Although the HIV transmission rate (β) has a low sensitivity index in this model, preventive measures like safe sex practices and needle exchange programs remain critical. Parameters like progression to AIDS (P), total population size (N), and AIDS population carrying capacity (K) have minimal sensitivity indices, suggesting limited direct influence on R_0.

Moderate negative sensitivity indices for ART progression rate (γ) and viral rebound rate (ν) emphasize the importance of ART access, adherence, and minimizing viral rebound to reduce R_0. HIV-induced death rate (μ_i), additional mortality due to HIV (δ_i), and progression to AIDS (λ) show modest negative indices, reflecting the role of ART in delaying disease progression and reducing transmission likelihood. These findings reinforce ART's central role in controlling HIV spread and the value of targeted public health interventions.

6. CONCLUSION

This study underscores Antiretroviral Therapy's (ART) crucial role in HIV transmission dynamics, highlighting its ability to reduce viral loads to undetectable levels and minimize transmission risk. Sensitivity analysis reveals that parameters such as treatment initiation rates and adherence significantly affect outcomes. Addressing barriers to ART access and adherence, especially among vulnerable populations, is vital for reducing HIV incidence. The findings support achieving UNAIDS 90-90-90 targets and emphasize integrating ART with behavioral interventions. This work provides critical insights for policymakers to enhance HIV prevention and treatment strategies, ensuring equitable and effective care access.

Key Findings

- Consistent ART adherence leads to undetectable viral loads, effectively minimizing transmission risk.
- The study demonstrates that ART is crucial in controlling HIV

transmission dynamics within populations.

- Findings support the integration of ART into public health strategies to achieve the UNAIDS 90-90-90 targets.
- Sensitivity analysis reveals that ART adherence rates and treatment initiation rates are critical determinants of treatment outcomes.
- Identifying and addressing barriers to ART access especially among vulnerable populations is essential for optimizing treatment outcomes.

Conflict of Interest: The authors declare that there is no conflict of interest regarding the publication of this research, and there are no personal or professional relationships that could be perceived as influencing the outcomes of this work.

References

Beyrer, C., Crago, A. L. and Bekker, L. G. (2023), 'The global HIV epidemic among sex workers: Progress and challenges', *The Lancet HIV* **10**(3), e144–e153.

Chang, L. W., Serwadda, D., Quinn, T. C. and Gray, R. H. (2023), 'The long-term impact of antiretroviral therapy on HIV transmission dynamics', *Journal of Acquired Immune Defciency Syndromes* **93**(4), 417–424.

Cohen, M. S., Chen, Y. Q., McCauley, M., Gamble, T., Hosseinipour, M. C., Kumarasamy, N. and Team, H. . S. (2011), 'Prevention of HIV-1 infection with early antiretroviral therapy', *New England Journal of Medicine* **365**(6), 493–505.

Delaney, K. P., Sanchez, T., Bowles, K., Oraka, E., DiNenno, E. and Finlayson, T. (2022), 'Declines in community-level HIV incidence with increased ART access: Evidence from the united states', *AIDS and Behavior* **26**(2), 486–497.

Garcia, M., Fernandez, E. and Perez, J. (2024), 'Socioeconomic factors and HIV risk behaviors: A systematic review', *Social Science and Medicine* **307**, 115242.

Grant, R. M., McMahon, J. H. and Liu, A. Y. (2023), 'Factors influencing PrEP uptake and adherence among young women in sub-saharan africa', *The Lancet HIV* **10**(1), e26–e35.

Jin, H., Wilson, E. and Baral, S. (2022), 'Addressing barriers to HIV prevention and care for transgender populations: Global perspectives', *Journal of the International AIDS Society* **25**(2), e25960.

Johnson, C. A., Wang, L. and Smith, D. (2022), 'Stigma, discrimination, and HIV access: Overcoming barriers to care', *Journal of AIDS and HIV Research* **14**(6), 198–209.

Jones, C. B., Sullivan, P. S. and Sanchez, T. H. (2024), 'Impact of community-based interventions on risky sexual behaviors among MSM: A systematic

review', *AIDS and Behavior* **28**(1), 12–24.

Kalichman, S. C., Eaton, L. A. and Cherry, C. (2023), 'COVID-19 disruptions to HIV prevention and treatment: Implications for public health', *Public Health Reports* **138**(2), 114–124.

Molina, J. M., Landovitz, R. J. and Delaugerre, C. (2022), 'Long-acting injectable PrEP for HIV prevention: Efcacy and safety outcomes', *New England Journal of Medicine* **387**(5), 387–399.

Nguyen, T. H., Falcone, V. and Hammer, S. M. (2024), 'Innovations in HIV vaccine development: A focus on mRNA-based approaches', *Nature Reviews Drug Discovery* **23**(3), 218–229.

Rodriguez, P., Martinez, J. and Lopez, A. (2022), 'The bidirectional relationship between HIV and tuberculosis: Integrated care approaches', *Journal of Infectious Diseases* **226**(1), S86–S93.

Schnall, R., John, R. M. and Carballo-Dieguez, A. (2023), 'Digital health interventions for HIV prevention: A meta-analysis of effectiveness', *Journal of Medical Internet Research* **25**(6), e38243.

Smith, A. E. and Wagner, B. (2023), 'ART in HIV-infected patients with cardiovascular disease: Review and management strategies', *Journal of Cardiovascular Medicine* **24**(2), 121–133.

Smith, L. R., Gomez, M. and Lightfoot, M. (2023), 'The impact of housing instability on HIV risk and prevention: Insights from recent research', *AIDS and Behavior* **27**(5), 1361–1370.

Wilson, I. B., Gerrity, M. and O'Brien, M. E. (2024), 'Gender-based violence and HIV transmission: Addressing the intersection to improve health outcomes', *AIDS Care* **36**(3), 283–295.

Zhang, Q., Liu, X. and Huang, Y. (2023), 'Artifcial intelligence in HIV prevention: Predicting transmission patterns and optimizing interventions', *Nature Reviews Drug Discover y* 22**(**9), 708–722.